JOURNAL OF SOLID STATE CHEMISTRY 73, 224–234 (1988)

Energetics of Brannerite-Type Solid Solutions: The Systems ZnV_2O_6–$LiMoVO_6$ and MgV_2O_6–$LiMoVO_6$

K. MOCALA* AND A. NAVROTSKY

Department of Geological and Geophysical Sciences, Princeton University, Princeton, New Jersey 08544

Received May 21, 1987; in revised form July 31, 1987

Enthalpies of mixing in brannerite-type solid solutions ZnV_2O_6–$LiMoVO_6$ and MgV_2O_6–$LiMoVO_6$ were determined by transposed temperature-drop solution calorimetry into a molten sodium molybdate solvent at 702°C. The ZnV_2O_6–$LiMoVO_6$ system shows zero heats of mixing (to ± 2 kJ/mole) and symmetrical negative excess volumes of mixing. The MgV_2O_6–$LiMoVO_6$ system shows more complex behavior, with positive enthalpies of mixing at MgV_2O_6-rich end and negative heats of mixing at $LiMoVO_6$-rich compositions. Volumes of mixing are negative at MgV_2O_6-rich compositions and essentially zero on the $LiMoVO_6$-rich side. This complex behavior suggests that several effects compete to result in the observed energetic and structural behavior. These factors may be (a) strain energy associated with size-mismatch, (b) the relaxation of rather long Mg–O bonds in MgV_2O_6 upon solid solution formation, and (c) the effect of simultaneous coupled substitution of Li on Mg sites and of Mo on V sites, possibly with some short-range order.

Introduction

Thermodynamic investigation of multicomponent solid solutions can bring new data to the development of the theory of solid solutions and can be useful from a practical point of view. Multicomponent solid solutions are used in modern electronic, optical, magnetic, and superconducting materials, and as selective model catalysts. This last application was developed in various catalytic laboratories using multicomponent solid solutions with scheelite (*1, 2*), perovskite (*3*), and brannerite (*4, 5*) structure types. In the present study we have concentrated on brannerite-type solid solutions.

The brannerite ($ThTi_2O_6$) structure (*6*) is monoclinic with the space group $C2/m$ or $C2$ (*7, 8*). This class of crystals (AX_2O_6) can be described as composed of distorted XO_6 octahedra with $X = Ti^{4+}$ or V^{5+} (Fig. 1). These octahedra share opposite corners forming chains running parallel to the b axis. Octahedra in adjacent chains share edges involving O(2)a and O(2)c sites on one side of the chain (Fig. 1c). On the other side, chains interleaf with two adjacent octahedra in a neighboring chain. These edges are O(3)a and O(3)g on one octahedron and O(3)a and O(3)g on the next one (translated by a "b" axis length).

A-type ions (Th, Mg, Ca, Mn, Co, Cu, Zn, Cd) lie in octahedral interstices sharing oxygen atoms with six different X atoms

* Permanent address: Institute of Catalysis and Surface Chemistry, Polish Academy of Sciences, ul. Niezopominajek, 30-239 Krakow, Poland.

0022-4596/88 $3.00

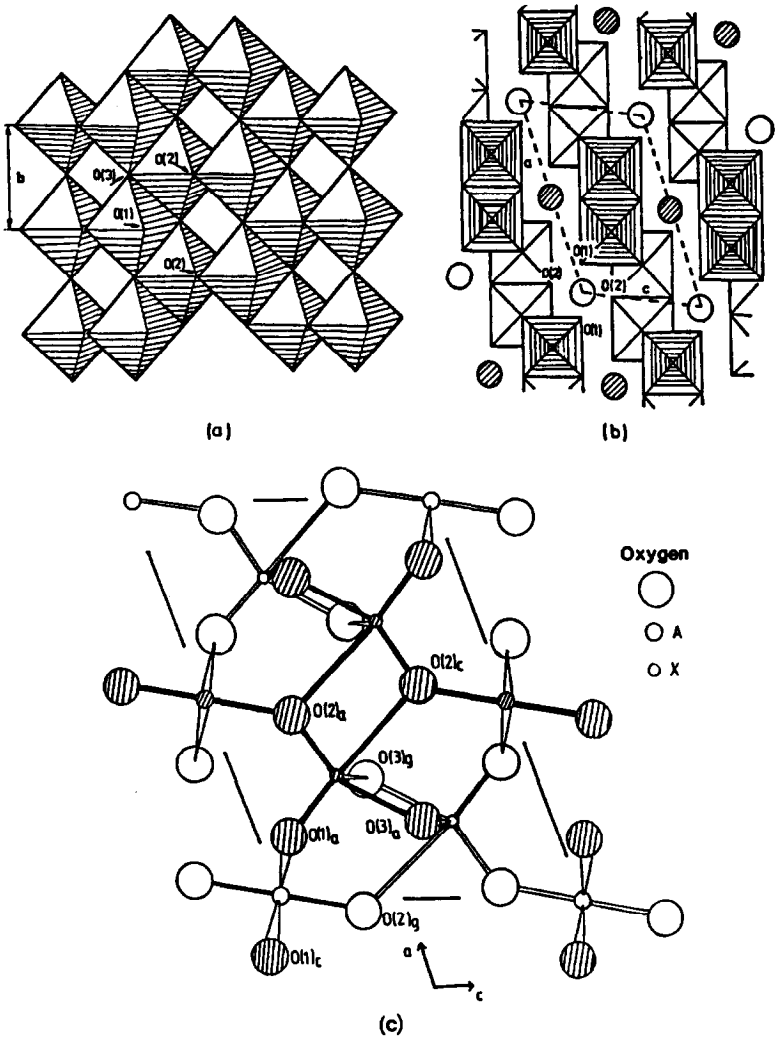

FIG. 1. Brannerite-type AX_2O_6 structure. (a) A sheet of XO_6 octahedra parallel to (001) plane (idealized outline). (b) Projection of the idealized structure on the *ac* plane with *A* cation and VO_6 octahedra marked at two different levels (shaded circles and octahedra at $y = \frac{1}{2}$). (c) Real AX_2O_6 structure (after 26) (shaded circles and darkened bonds at $y = \frac{1}{2}$; unshaded at $y = 0$).

from the two neighboring vanadium layers. AO_6 groups form chains paralleling the *b* axis by sharing O(1)a–O(1)c edges with two translation-equivalent AO_6 groups.

This structure is amenable to substitution of other cations either by appropriate cation substitution or by vacancy formation on *A*-type sites if charge balance is maintained. Several metavanadates form solid solutions with MoO_3 and Li_2O. These solid solutions have the general formula (*8–14*):

$$A\mathrm{Li}\phi = A_{1-x-y}\phi_x\mathrm{Li}_y\mathrm{V}_{2-2x-y}\mathrm{Mo}_{2x+y}\mathrm{O}_6$$
$$A = \mathrm{Mn, Co, Zn, Mg, Cu.} \quad (1)$$

In this series Mo^{6+} ions substitute randomly for V^{5+} ions; similarly Li^+ and cation vacancies ϕ substitute for A^{2+} ions. The extreme cases of $A\mathrm{Li}\phi$ are: $A\phi = A_{1-x}\phi_x$

$V_{2-2x}Mo_{2x}O_6$ (at $y = 0$), $A\text{Li} = A_{1-y}\text{Li}_y$ $V_{2-y}Mo_yO_6$ (at $y = 0$), and $\text{Li}\phi = \text{Li}_{1-x}$ $\phi_xV_{1-x}Mo_{1+x}O_6$ (at $x + y = 1$) (*15*). The first case is a solid solution between AV_2O_6 and MoO_3, the second case is between AV_2O_6 and $LiVMoO_6$ (also a compound with brannerite structure), and the last case is between $LiVMoO_6$ and MoO_3. $A\text{Li}\phi$ may be considered as an ALi matrix doped with an excess of MoO_3 where excess Mo^{6+} ions are compensated by cation vacancies ϕ. The phase diagrams and lattice parameters were published recently for solid solutions with Mn, Zn, Mg, and Co as A^{2+} ions (*9, 10, 12–14*). Mocala and Ziolkowski (*13, 14*) have argued that the observed negative deviations from Vegard's Law for ZnLi and MgLi solid solutions suggest an unexpected stabilization of the crystal structure by substitution of monovalent (Li^+) ions for divalent ions (Mg^{2+} or Zn^{2+}), thereby increasing its tolerance to cation vacancies. Effects of the simultaneous substitution of Mo^{6+} for V^{5+} in the vanadium layers were considered less important due to the layer structure of brannerite.

The purpose of the present research was to obtain thermodynamic data for ZnLi and MgLi solid solutions. In particular, we wished to test whether the proposed apparent stabilization of the crystal structure led to measurable deviations from ideal mixing in the solid solutions. High-temperature calorimetric techniques, see below, were used to obtain enthalpies of mixing in the MgV_2O_6–$LiMoVO_6$ and ZnV_2O_6–$LiMoVO_6$ solid solution series. Lattice parameters were also measured using an automated X-ray powder diffractometer.

Experimental

Sample Preparation

All samples used in the present investigation were the same as in previous studies (*13, 14*). They were synthesized by the amorphous citrate precursor method (*16*) adapted to these systems (*10*). Elemental analyses, atomic absorption spectroscopy, and classical flame photometry (for Li) of some selected samples proved a stoichiometry within ±1% in the absolute weight of the metals. The samples were dried at 120°C for 20–24 hr and were stored in a desiccator. MgV_2O_6 and MgLi solid solutions rich in that component were kept at room temperature in closed small vials immediately prior to calorimetric measurements to minimize water pickup due to the hygroscopicity of MgV_2O_6.

X-ray Measurements

X-ray measurements were performed on a Scintag Pad V automatic diffractometer using Cu$K\alpha$ radiation and a solid-state detector. A goniometer scan rate of 1° 2θ/min and chopper increment 0.02° 2θ were chosen. Background corrections were done by stripping the $K\alpha_2$ peaks. Peak positions were corrected and calculated using the first four lines of Al ($a = 4.0494$ Å at 23°C) as an internal standard. The lattice dimensions were refined by a version of the Appelman and Evans least-squares procedure (*17*) using 15–25 reflections.

Calorimetric Measurements

The goal of the calorimetric measurements was to dissolve the samples reproducibly in a molten oxide solvent at high temperature. Preliminary experiments showed that the brannerites dissolved readily in molten sodium molybdate, $3Na_2O \cdot 4MoO_3$, near 700°C. This solvent has been used previously for solution calorimetry of binary and ternary oxides containing divalent ions, Ti^{4+}, Sn^{4+} (*18, 19*). However, the brannerite solid solutions cannot be maintained at 700°C because of phase transitions to high-temperature polymorphs and/or melting reactions. Therefore solution calorimetry, requiring several hours of preequilibration at calorimetric temperature, could not be used. Instead, transposed tem-

perature-drop solution calorimetry, in which the sample is dropped from room temperature into the solvent in the calorimeter at high temperature, was used. The heat effect measured is then the sum of a heat content (H_{702}–H_{23}) and heat of solution. The advantage of the method lies in its ability to handle samples not stable for long periods at calorimetric temperature. Its disadvantage (see below) is in the large magnitude of the heat effects measured.

The twin Calvet-type microcalorimeter (*20*), calibrated by the Pt-drop method (*21*), was used at 702°C. Samples weighing 20–30 mg, held in small cups (0.1 in. diameter and 0.45 to 0.5 in. long) of 0.0005-in.-thick Pt foil were equilibrated at room temperature and were dropped and dissolved in ~13.0 g of molten sodium molybdate, $3Na_2O \cdot 4MoO_3$. The solvent was held in Pt crucibles and was used for three dissolutions. Samples dissolved readily and gave complete reaction times of typically 35 min before a steady baseline was restored. Measured enthalpies were ~20 J and consisted of the heat content of Pt, the heat content of the sample, and the heat of solution of the sample. The heat content of the Pt capsule contributed 15–20% to the total heat effect. The observed heat effects were endothermic throughout each run. Occasional experiments, in which the capsule did not fall straight into the melt and the sample did not dissolve completely, gave erratic results and were discarded.

Two separate series of experiments were done, one on the Mg–Li solid solution and one on Zn–Li. The molar enthalpies observed (sum of heat content and heat of solution) were in the range 170–195 kJ/mole with errors (two standard deviations of the mean) of 0.9 to 2.6 kJ/mole (0.6 to 1.4%). The Mg–Li system gave slightly smaller standard deviations with somewhat fewer experiments. $LiVMoO_6$ was measured during both sets of experiments, giving 194.9 (±1.2) kJ/mole for 20 experiments (ZnLi series) and 194.5 (±0.5) kJ/mole for 5 experiments (MgLi series). A final average of 194.8 (±1.0) kJ/mole from all experiments was used for $LiVMoO_6$ in both systems.

Because the enthalpies of mixing (see below) are derived from the difference in observed enthalpies of the solid solutions and the weighted average of the end members, it is necessary to make certain that the observed enthalpies are indeed independent of the concentration of dissolved components in the flux. To check that this infinitely dilute or Henry's law limit was applicable, a number of experiments were done in which, in a series of three samples dissolved in the same solvent, the composition of each subsequent sample was varied. Within the uncertainties given above, there was no difference in the enthalpy of, for example, MgV_2O_6 dissolved as the first sample in the flux, as a second or third sample in a flux containing MgV_2O_6, or in a flux containing $LiVMoO_6$.

Results

X-ray Investigations

Our X-ray patterns for ZnLi and MgLi solid solutions show that the samples are monophasic with a brannerite-type structure. Sample ZnLi, $y = 0.47$, which had small amounts of impurities, was eliminated from further investigation. Calculated lattice parameters for ZnLi solid solutions are given in Table 1 and are compared with previously published results (Fig. 2). Lattice parameters for MgLi are given in Table 1 and are plotted with other published data in Fig. 3. The curves on Figs. 2 and 3 are visual fits to the data. The agreement of our results with previous data is good.

Lattice parameters "a" and "b" for ZnLi solid solutions change practically linearly with composition. Parameter "c," angle β, and $c \sin \beta$ change in a nonlinear and even nonmonotonic manner along the ZnLi series. This results in a negative deviation

TABLE I

LATTICE PARAMETERS FOR THE $ALi = A_{1-y}Li_yV_{2-y}Mo_yO_6$ SOLID SOLUTIONS (A = Zn, Mg)

	a (Å)	b (Å)	c (Å)	β (deg)	$c \sin\beta$ (Å)	V (Å^3)
ZnV_2O_6	9.2408(4)[a]	3.5261(2)	6.5702(3)	111.353(3)	6.1192	199.38(1)
ZnLi y = 0.10	9.2478(15)	3.5392(8)	6.5647(10)	111.460(12)	6.1096	199.97(5)
ZnLi y = 0.20	9.2617(14)	3.5547(7)	6.5677(8)	111.580(12)	6.1073	201.07(4)
ZnLi y = 0.35	9.2777(9)	3.5741(5)	6.5711(9)	111.678(9)	6.1064	202.50(3)
ZnLi y = 0.40	9.2771(18)	3.5776(12)	6.5740(16)	111.714(21)	6.1075	202.71(6)
ZnLi y = 0.53	9.2940(11)	3.5900(12)	6.5835(11)	111.745(11)	6.1150	204.03(5)
ZnLi y = 0.60	9.2959(11)	3.5975(11)	6.5848(17)	111.743(14)	6.1163	204.54(6)
ZnLi y = 0.80	9.3186(14)	3.6220(8)	6.6045(14)	111.728(16)	6.1353	207.08(5)
$LiVMoO_6$	9.3418(5)	3.6449(3)	6.6342(5)	111.636(6)	6.1668	209.98(2)
MgLi y = 0.90	9.3365(13)	3.6367(13)	6.6431(6)	111.783(9)	6.1687	209.45(3)
MgLi y = 0.80	9.3277(28)	3.6231(11)	6.6445(16)	111.911(21)	6.1645	208.33(8)
MgLi y = 0.60	9.3133(18)	3.6017(13)	6.6533(17)	112.121(20)	6.1635	206.75(7)
MgLi y = 0.50	9.3090(13)	3.5889(11)	6.6563(11)	112.122(11)	6.1662	206.01(5)
MgLi y = 0.40	9.2962(9)	3.5678(6)	6.6683(9)	112.185(8)	6.1746	204.79(3)
MgLi y = 0.20	9.2767(21)	3.5296(6)	6.6889(8)	112.168(15)	6.1945	202.82(5)
MgLi y = 0.10	9.2824(16)	3.5106(4)	6.7071(8)	111.998(8)	6.2188	202.65(3)
MgV_2O_6	9.2807(12)	3.4886(4)	6.7309(7)	111.762(11)	6.2512	202.39(3)

[a] Estimated standard deviation.

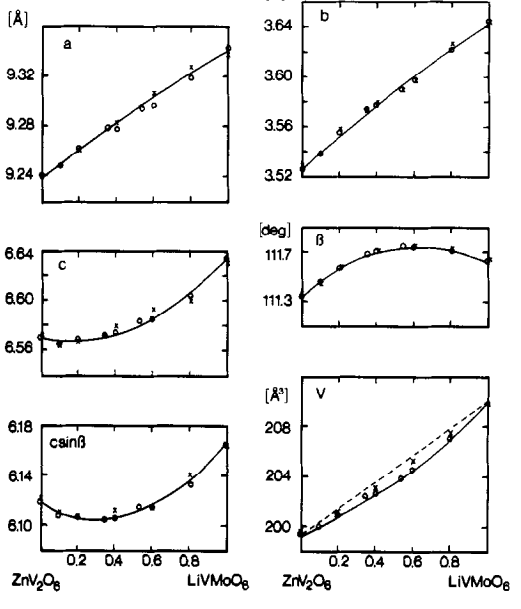

FIG. 2. Lattice parameters of ZnLi solid solutions as function of composition. Circles, present results (errors, see Table 1); crosses, data after (*13*). A dashed line is drawn between the unit cell volumes of the two end members.

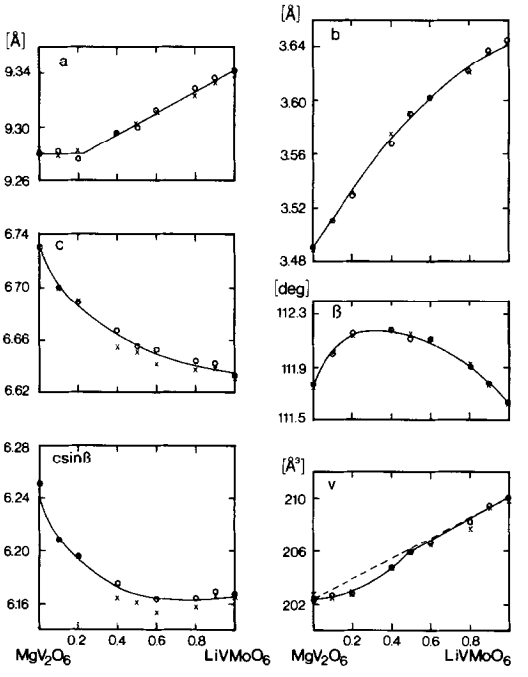

FIG. 3. Lattice parameters of MgLi solid solutions as a function of composition. Circles, present results (errors, see Table 1); crosses, data after (*14*). A dashed line is drawn between the unit cell volumes of the two end members.

from linearity with composition for the unit cell volume V. Our present results show even slightly larger deviations than previously obtained, especially for samples with high concentration of $LiVMoO_6$.

All lattice parameters in the MgLi solid solutions change in a nonlinear fashion with composition, showing both negative and positive deviations from Vegard's Law. Discussions of the changes in lattice dimensions for ZnLi and MgLi solid solutions were presented elsewhere (*13, 14*) and take into account sizes of dopant ions and compactness of the brannerite structure in various directions. Such discussion can predict the directions of changes of lattice parameters with composition but not the deviations from ideality. It cannot explain the peculiar relations between lattice dimensions and composition for several cases (e.g., constant or even slightly decreasing "a" parameter in the range $y = 0$–0.25 for MgLi).

Figures 5a and 5b present the calculated volume of mixing ΔV_{mix} for ALi (A = Zn, Mg) according to the equation:

$$\Delta V_{mix} = V_{ALi} - yV_{LiVMoO_6} - (1 - y)V_{AV_2O_6}. \quad (2)$$

Error bars represent two standard deviations of the mean for ΔV_{mix} calculated from the propagation of errors (also 2σ) for unit cell volumes of AV_2O_6, $LiVMoO_6$, and ALi solid solutions, where A = Mg, Zn. The negative deviation from ideal volume of mixing is similar in magnitude for both systems. The ZnLi system shows negative volumes of mixing over the entire composition range, with the largest deviation from ideality at $y \simeq 0.60$. The MgLi system shows negative excess volumes for $y < 0.5$ (largest deviation near $y = 0.25$) and virtually zero volumes of mixing for $y > 0.5$.

Calorimetric Results

ZnLi = $Zn_{1-y}Li_yV_{2-y}Mo_yO_6$ solid solutions. Results of transposed drop solution calorimetry for ZnLi solid solutions are given in Table 2, together with the heats of mixing. The observed enthalpies (sum of heat content and heat of solution) for the two end members and seven solid solution compositions are fit by the equation

$$H_{ZnLi} = 170.4(\pm 0.75) + 24.6(\pm 1.4)y(\text{kJ/mole}), \quad (3)$$

where y = mole fraction $LiVMoO_6$, with a correlation coefficient of 0.989. The observed enthalpy data are shown in Fig. 4a, where the error bars are two standard deviations of the mean. The calculated line virtually overlaps the straight line connecting the observed enthalpies of the two end members. A quadratic fit to the data is statistically unwarranted. Figure 5c shows the heat of mixing, calculated from

$$\Delta H_{mix} = yH_{LiVMoO_6} + (1 - y)H_{ZnV_2O_6} - H_{ZnLi}. \quad (4)$$

The error bars on ΔH_{mix} are calculated by propagation of errors in the measured enthalpies. Within experimental error (about ± 2 kJ/mole), the ZnLi solid solutions are energetically ideal; they have a zero heat of mixing (at room temperature).

MgLi = $Mg_{1-y}Li_yV_{2-y}Mo_yO_6$ solid solutions. Results of transposed temperature-drop solution calorimetry for MgLi solid solutions are given in Table 2. The observed enthalpy and the enthalpy of mixing are shown in Figs. 4b and 5d. In contrast to the Zn–Li system, the MgLi system shows a definite deviation from ideal enthalpy behavior. There are negative heats of mixing for $y > 0.4$ and there may be small positive heats of mixing at $y < 0.2$. The observed enthalpy was fitted by least squares to a third-order polynomial giving the expression,

$$H_{obs} = 169.5(\pm 0.6) + 17.4(\pm 6.2)y + 39.7(\pm 15.3)y^2 - 31.9(\pm 10.1)y^3(\text{kJ/mole}), \quad (5)$$

TABLE II

RESULTS OF TRANSPOSED DROP SOLUTION CALORIMETRY, HEAT OF MIXING AND VOLUME OF MIXING FOR $A\text{Li} = A_{1-y}\text{Li}_y\text{V}_{2-y}\text{Mo}_y\text{O}_6$ SOLID SOLUTIONS (A = Zn, Mg)

	H_{obs} (kJ/mol)	ΔH_{mix}[a] (kJ/mol)	ΔV_{mix}[a] (cm³/mol)
ZnV_2O_6	170.0 ± 1.0[b](22)[c]	0	0
ZnLi y = 0.10	174.5 ± 2.2 (9)	−2.0 ± 2.4[b,d]	−0.14 ± 0.03[b,d]
0.20	173.9 ± 1.6 (13)	+1.1 ± 1.8	−0.13 ± 0.03
0.35	178.0 ± 1.9 (12)	+0.7 ± 2.0	−0.18 ± 0.02
0.40	181.9 ± 1.8 (9)	−2.0 ± 1.9	−0.28 ± 0.04
0.53	182.0 ± 2.1 (8)	−1.15 ± 2.2	−0.29 ± 0.04
0.60	186.0 ± 2.1 (8)	−1.1 ± 2.2	−0.36 ± 0.04
0.80	190.3 ± 1.3 (6)	−0.4 ± 1.5	−0.23 ± 0.03
$LiVMoO_6$	194.8 ± 1.0 (25)	0	0
MgLi y = 0.90	194.4 ± 1.3 (5)	−2.1 ± 1.6	+0.07 ± 0.02
0.80	191.55 ± 1.4 (5)	−1.8 ± 1.65	−0.04 ± 0.05
0.60	188.4 ± 1.7 (5)	−3.6 ± 1.8	−0.06 ± 0.05
0.50	184.1 ± 2.6 (6)	−1.8 ± 2.7	−0.05 ± 0.03
0.40	180.4 ± 0.9 (7)	−0.7 ± 1.2	−0.19 ± 0.02
0.20	174.4 ± 0.9 (5)	+0.2 ± 1.4	−0.32 ± 0.03
0.10	171.45 ± 2.2 (5)	+0.7 ± 2.5	−0.15 ± 0.02
MgV_2O_6	169.6 ± 1.2 (5)	0	0

[a] Values calculated from Eqs. (4) and (2), respectively.
[b] Two standard deviation of the mean.
[c] Number of experiments.
[d] Calculated from the propagation of errors for AV_2O_6, $LiVMoO_6$, and ALi solid solutions.

with y mole fraction of $LiVMoO_6$ and correlation coefficient 0.998. The enthalpy of mixing and enthalpy interaction parameter

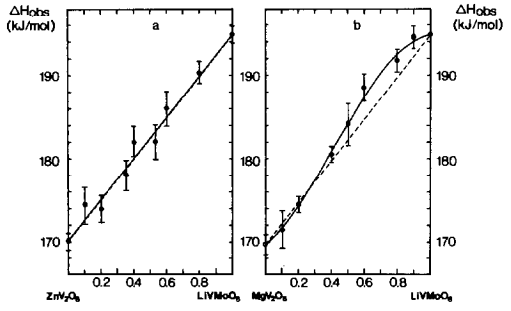

FIG. 4. Observed enthalpies H_{obs} (heat content and heat of solution) of ZnLi (a) and MgLi (b) solid solutions. Error bars, two standard deviations of the mean. Dashed lines are between end members; solid curves represent Eqs. (3) and (5), respectively.

were obtained directly from H_{obs} values by regression of a function defined by,

$$H_{obs} = Ay + B(1 - y) - y(1 - y)[C + Dy]$$
$$= B + (A - B)y - y(1 - y)[C + Dy], \quad (6)$$

where the first two terms represent ideal mixing between MgV_2O_6 and $LiVMoO_6$ and the last term represents the enthalpy of mixing. The curves representing enthalpy of mixing, ΔH_{mix}, and enthalpy interaction parameter, λ_H, plotted in Figs. 5d and 5e are given by the expressions:

$$\Delta H_{mix} = y(1 - y)\lambda_H \quad (7)$$

and

$$\lambda_H = 7.8(\pm 5.6) - 31.9(\pm 10.0)y. \quad (8)$$

Experimental points for the enthalpy of mixing and enthalpy interaction parameter

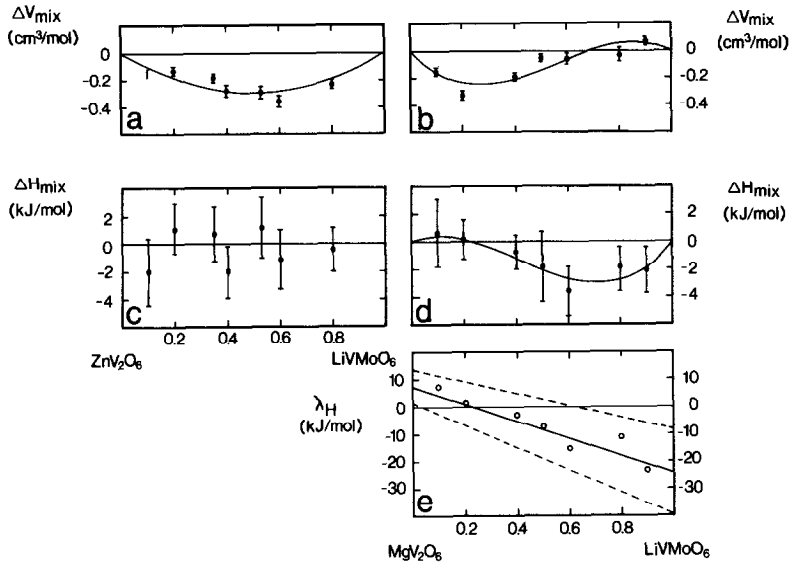

FIG. 5. (a) Volume of mixing ΔV_{mix} as a function of composition for ZnLi solid solutions calculated from Eq. (2). Least-squares curve is represented by the equation $\Delta V_{mix} = (-1.17 \pm 0.09)y(1 - y)$ cm³/mole (regular model). (b) Volume of mixing (Eq. 2) as a function of composition for MgLi solid solutions. Least-squares curve is represented by a two-parameter equation: $\Delta V_{mix} = 3.00(\pm 0.35)(y)(1 - y)[y - 0.69(\pm 0.22)]$ cm³/mole. (c) Enthalpy of mixing ΔH_{mix} of ZnLi solid solutions calculated from Eq. (4). (d) Enthalpy of mixing ΔH_{mix} of MgLi solid solutions calculated from Eq. (4). Least-squares curve is represented by Eq. (5). (e) Dependence of the enthalpy interaction parameter λ_H vs composition for MgLi solid solutions. Experimental points calculated from Eq. (7). The least-squares line is given by Eq. (8). Dashed lines represent the lines with the maximum error in coefficients for Eq. (8). Error bars (for a–d), two standard deviations of the mean calculated from propagation of errors (also 2σ) for AV_2O_6, $LiVMoO_6$, and ALi solid solutions (A = Zn, Mg).

are taken from Table 2 and calculated from Eq. (7), respectively. As can be seen from Fig. 5e, a linear relationship between enthalpy interaction parameter λ_H and composition seems to be reasonable. The dashed lines represent the uncertainty in λ_H estimated from the errors of the coefficients in Eq. (7).

To our knowledge there are no direct experimental values for λ_H in infinite dilution for MgV_2O_6 and $LiVMoO_6$ in the literature. We believe that extrapolation of Eq. (8) to the end members can give approximate values for these quantities. Recently, Capobianco and Navrotsky (*22*) have shown that for the $CaCO_3$–$MnCO_3$ system, such extrapolations give results comparable to values obtained from activity coefficient data derived from phase equilibrium experiments. Extrapolation of Eq. (8) shows that the interaction parameter changes from 7.8(±5.6) kJ/mole^{-1} for $LiVMoO_6$ dissolving at infinite dilution in MgV_2O_6 to −24.1 ± 15.6 kJ/mole^{-1} for MgV_2O_6 dissolving in $LiVMoO_6$. The solid solution with $y = 0.24$ appears ideal with $\lambda_H = 0$.

Discussion

The present data show that the relation between excess enthalpy and excess volume in the MgLi and ZnLi systems is not

simple. The ZnLi system shows essentially zero heat of mixing and negative volume of mixing throughout all compositions. The MgLi system shows large negative volumes of mixing at $y < 0.4$ and almost zero volumes of mixing at $y > 0.4$ with ΔH_{mix} zero or slightly positive at $y < 0.4$ and significantly negative at $y > 0.4$. Figure 6 shows the relation between the enthalpy interaction parameter, λ_H, and volume interaction parameter, λ_V, for the two systems. The volume and enthalpy data are taken from Table 2, with $\lambda_V = \Delta V_{mix}/(y(1 - y))$ and $\lambda_H = \Delta H_{mix}/(y(1 - y))$ for MgLi system. For ZnLi, the average value of λ_V is -1.17 (± 0.09) cm^3/mole, the average value of λ_H is zero. λ_V for ZnLi system was calculated by fitting the ΔV_{mix} data (from Table 2) to a regular model $\Delta V_{mix} = y(1 - y)\lambda_V$. The MgLi system shows much more asymmetry, with λ_V and λ_H calculated from the volumes of mixing and enthalpy of mixing at each composition. Figure 6 shows the correlation between λ_V and λ_H. Despite considerable scatter a clear trend is seen; as ΔV_{mix} and λ_V become less positive, λ_H becomes more positive and passes through zero near $\lambda_V = -1.25$ cm^3/mole. The ZnLi data point ($\lambda_H = 0$, $\lambda_V = -1.17(\pm 0.09)$ cm^3/mole) falls near the trend defined by the MgLi data.

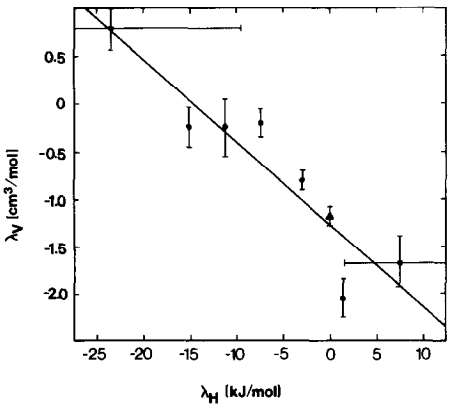

FIG. 6. A relation between the enthalpy interaction parameter λ_H and volume interaction parameter λ_V for ALi solid solutions (A = Zn, Mg). Points represent the data for MgLi system; a triangle represents the data for ZnLi system. Vertical error bars represent the two standard deviations of the mean (MgLi system) and uncertainty of regular model; see text and Fig. 5a (ZnLi system) for λ_V. The horizontal bars represent estimated errors of λ_H from Fig. 5c (only for two extreme samples).

How can one explain these observations on crystal chemical grounds? It is known that the MgV_2O_6 unit cell volume is bigger than one would expect by comparison with other vanadates (*14, 23*). A larger unit cell volume can result from a misfit of the vanadium layers with respect to one another. Although the ionic radius of Mg^{2+} in octahedral coordination is 0.72 Å (*24*), in the MgV_2O_6 the average Mg–O distance implies an effective Mg^{2+} radius of 0.78 Å (*25, 26*). Apparently the Mg cations that lie in the octahedral interstices between two neighboring vanadium layers do not interact strongly enough with oxygens from the vanadium layers to force the Mg–O distances to be those typical for other magnesium–oxygen bonds. In this sense, MgV_2O_6 may be thought of as an unrelaxed structure. Deviation from ideal volumes for MgLi results mainly from the deviations in the a and c sin β parameters. As can be seen from Fig. 3, a is practically constant to $y = 0.22$ despite the substitution of normally larger ions: Mo^{6+} (0.59 Å) and Li^+ (0.76 Å) for smaller ions V^{5+} (0.54 Å) and Mg^{2+} (0.72 Å). The c sin β parameter actually decreases strongly to $y = 0.40$ and then changes only slightly to $LiVMoO_6$ (*24*). The constant value of the parameter a for $y < 0.22$ may be explained by the substitution of ions into the unrelaxed matrix. An increase in a is observed for $y > 0.22$. This change in the behavior of a occurs very near where the enthalpy interaction parameter, λ_H, goes through zero, see Fig. 5e. The substitution of Li^+ and Mo^{6+} for Mg^{2+} and Mo^{6+} changes the other lattice dimensions. These changes may help absorb the strain related to keeping a constant a dimension. Near $y = 0.22$, the size of the AO_6

octahedron (which may be partially constrained by constant a dimension) (A = Mg, Li) may be optimum for that composition's mixture of Mg and Li. Further substitution of larger ions causes a normal increase in a. The enthalpy of mixing is positive when a is constant and becomes negative when the structure is "relaxed."

These somewhat irregular changes in lattice parameters must affect the coordination polyhedra around the A-type ions. The point symmetry of the Mg site in MgV_2O_6 is $2/m$ with four Mg–O bonds of 2.198 Å and two of 2.024 Å. A further decrease of the symmetry of the A-cation site to point group 2 is possible, resulting in the separation of the four equal coplanar A–O bonds into two pairs with different bond lengths. This lower symmetry is characteristic of ZnV_2O_6 (*7*) and $Mn_{1-x}\phi_xV_{x-2x}Mo_{2x}O_6$ at x = 0.53 (*8*). Unfortunately, crystal structure refinements are not available for $LiMoVO_6$ and the ZnLi and MgLi solid solution series. It is possible that the substitution of Li + Mo for Mg + V lowers the space group symmetry from $C2/m$ to $C2$ and the A-site symmetry from $2/m$ to 2. No change in symmetry would occur during the substitution of Li + Mo for Zn + V because ZnV_2O_6 already has the lower symmetry. The complex behavior, in terms of lattice parameters and heats of mixing, of the MgLi substitution may then reflect the change in symmetry, perhaps even as a second-order transition. Further structural studies, perhaps by neutron diffraction, are needed to clarify this point.

There is no evidence that the substitution of Zn + V by Li + Mo causes any further lowering of symmetry. Such a transformation from monoclinic to triclinic symmetry would lead to peak splittings in the powder pattern of the ZnLi solid solutions, which were not observed.

Davies and Navrotsky (*27*) discussed the systematic behavior of enthalpies of mixing in binary and pseudobinary systems. They found that the magnitude of the positive interaction parameter could generally be related to volume mismatch, but that molybdate ($AMoO_4$) and tungstate (AWO_4) systems were anomalous in that a roughly constant positive enthalpy interaction parameter was seen regardless of which ions (divalent species or Mo and W) were being mixed. These compounds crystallize at atmospheric pressure with either a wolframite or a scheelite structure; the type of structure adopted depends upon the ionic radius of the divalent cation (*28*). In the scheelite and brannerite structure, the MoO_6, WO_6, and/or VO_6 polyhedra are the most rigid and well-defined structural elements, in terms of constant geometry and strongest bonding. Thus any structural relaxation or change which occurs upon substitution presently involves mainly the other polyhedra. Perhaps under this constraint of rigidity, the rest of the structure cannot adapt as easily to changes in other bond lengths, thus resulting in larger positive deviations from ideality, for a given size mismatch, than in solid solutions where all polyhedra contain bonds of more equal strength. The MgLi brannerite series for low concentrations of $MgLiVO_6$ appears to follow a trend similar to that in the wolframite and scheelite structures.

The next question is why the enthalpy interaction parameter λ_H for MgLi solid solutions decreases to zero and even negative values with increasing $LiVMoO_6$ concentration, while substitution in the scheelite and wolframite structures apparently always results in a positive interaction parameter for all compositions. In other words, why does substitution into the scheelite and wolframite structures always destabilize the structure, while stabilization is observed for a range of MgLi brannerite solid solutions? The main difference may be that for the scheelite and wolframite structures substitution is only into one sublattice (A^{2+} or X^{6+}), while for the branner-

ite MgLi solid solutions substitution occurs on both sublattices simultaneously. The relaxation of the anomalously long Mg–O bond lengths when $LiMoVO_6$ is added may also play a role. It is possible that other effects, for example, short-range ordering of the –V–O–Li–O–Mo– clusters, can stabilize the solid solutions. Such short-range order would maintain local charge balance during the substitution. However, there is no direct evidence for either short-range or long-range order in the brannerite solid solutions or compounds. Kozlowski and Stadnicka (*8*) have postulated randomly distributed Mo–O–ϕ–O–Mo (ϕ-vacancy) clusters in the brannerite solid solutions $Mn_{1-x}\phi_xV_{2-2x}Mo_{2x}O_6$, $x = 0.53$, based on bond length–bond strength calculations.

Neither our X-ray powder data nor single-crystal data for the $Mn_{1-x}\phi_xV_{2-2x}Mo_{2x}O_6$ ($x = 0.53$) and $NaVMoO_6$ (*29*) show evidence for superstructure formation. Darriet and Galy (*29*) have discussed several hypotheses for vanadium and molybdenum distributions in the $NaVMoO_6$ unit cell. Statistical distribution of vanadium and molybdenum ions over the x position was chosen as the best description of the experimental results. However, neither investigation looked at samples cooled slowly to low temperatures. Further investigation by high-resolution transmission electron microscopy and neutron diffraction may bring new results.

Acknowledgment

This work was supported by the Solid State Chemistry Program of the National Science Foundation (Grant DMR 8610816).

References

1. A. W. Sleight, *in* "Advanced Materials in Catalysis" (J. J. Burton and R. L. Garten, Eds.), Academic Press, New York (1977).
2. J. F. Brazdil, L. C. Glaeser, and R. K. Grasselli, *J. Catal.* **8,** 142 (1983).
3. R. J. H. Voorhoevc, J. P. Remeika, and L. E. Trimble, *in* "The Catalytic Chemistry of Nitrogen Oxides" (R. L. Kimisch and J. G. Larson, Eds.), p. 215, Plenum, New York (1977).
4. J. Ziolkowski and J. Janas, *J. Catal.* **81,** 298 (1983).
5. J. Ziolkowski and M. Gasior, *J. Catal.* **84,** 74 (1983).
6. B. Ruh and A. D. Wadsley, *Acta Crystallogr.* **21,** 974 (1968).
7. J. Angenault, *Rev. Chim. Miner.* **7,** 651 (1970).
8. R. Kozlowski and K. Stadnicka, *J. Solid State Chem.* **39,** 271 (1981).
9. R. Kozlowski, J. Ziolkowski, K. Mocala, and J. Haber, *J. Solid State Chem.* **35,** 1 (1980); Erratum **38,** 138 (1981).
10. J. Ziolkowski, K. Krupa and K. Mocala, *J. Solid State Chem.* **48,** 376 (1983).
11. T. Machej, R. Kozlowski and J. Ziolkowski, *J. Solid State Chem.* **38,** 97 (1981).
12. K. Mocala, J. Ziolkowski, and L. Dziembaj, *J. Solid State Chem.* **56,** 84 (1985).
13. K. Mocala and J. Ziolkowski, *J. Solid State Chem.* **71,** 426 (1987).
14. K. Mocala and J. Ziolkowski, *J. Solid State Chem.* **71,** 552 (1987).
15. J. Galy, J. Darriet, and B. Darriet, *C. R. Acad. Sci., Paris Ser. C* **264** (1967).
16. P. Courty, H. Ajot, and C. Marcilly, *Powder Technol.* **7,** 21 (1973).
17. D. E. Appelman and H. T. Evans, U. S. Department of Commerce, National Technology Information Service, Pb 216 188, Job 921A (1973).
18. B. A. Wechsler and A. Navrotsky, *J. Solid State Chem.* **55,** 165 (1984).
19. A. Navrotsky and R. B. Kasper, *Earth Planet Sci. Lett.* **31,** 247 (1976).
20. A. Navrotsky, *Phys. Chem. Miner.* **2,** 89 (1977).
21. O. J. Kleppa, *Colloq. Int. C. N. R. S.* **201,** 119 (1972).
22. C. Capobianco and A. Navrotsky, *Amer. Miner.* **72,** 312 (1987).
23. M. Gondrand, A. Collomb, J. C. Joubert, and R. D. Shannon, *J. Solid State Chem.* **11,** 1 (1974).
24. R. Shannon, *Acta Crystallogr. A* **32,** 751 (1976).
25. K. Mocala and J. Ziolkowski, *J. Solid State Chem.* **69,** 299 (1987).
26. H. N. Ng and C. Calvo, *Canad. J. Chem.* **50,** 3619 (1972).
27. P. K. Davies and A. Navrotsky, *J. Solid State Chem.* **46,** 1 (1983).
28. A. W. Sleight, *Acta Crystallogr. Sect. A* **28,** 2899 (1972).
29. B. Darriet and J. Galy, *Bull. Soc. Fr. Miner. Cristallogr.* **91,** 325 (1968).